

This paper was presented at a colloquium entitled "Molecular Recognition," organized by Ronald Breslow, held September 10 and 11, 1992, at the National Academy of Sciences, Washington, DC.

Toward an estimation of binding constants in aqueous solution: Studies of associations of vancomycin group antibiotics

(amide–amide hydrogen bond strengths/hydrophobic effect/rotor restrictions/enthalpy/entropy compensation/enthalpic barriers)

DUDLEY H. WILLIAMS, MARK S. SEARLE, JOEL P. MACKAY, UTE GERHARD, AND RACHEL A. MAPLESTONE

University Chemical Laboratory, Lensfield Road, Cambridge CB2 1EW, United Kingdom

ABSTRACT An approach toward the estimation of binding constants for organic molecules in aqueous solution is presented, based upon a partitioning of the free energy of binding. Consideration is given to polar and hydrophobic contributions and to the entropic cost of rotor restrictions and bimolecular associations. Several parameters (derived from an analysis of entropy changes upon the melting of crystals and from the binding of cell wall peptide analogues to the antibiotic ristocetin A) which may be useful guides to a crude understanding of binding phenomena are presented: (i) amide–amide hydrogen bond strengths of $-(1 \text{ to } 7) \pm 2 \text{ kJ}\cdot\text{mol}^{-1}$, (ii) a hydrophobic effect of $-0.2 \pm 0.05 \text{ kJ}\cdot\text{mol}^{-1}\cdot\text{\AA}^{-2}$ of hydrocarbon removed from exposure to water in the binding process, and (iii) free energy costs for rotor restrictions of $3.5\text{--}5.0 \text{ kJ}\cdot\text{mol}^{-1}$. The validity of the parameters for hydrogen bond strengths is dependent on the validity of the other two parameters. The phenomenon of entropy/enthalpy compensation is considered, with the conclusion that enthalpic barriers to dissociations will result in larger losses in translational and rotational entropy in the association step. The dimerization of some vancomycin group antibiotics is strongly exothermic (-36 to $-51 \text{ kJ}\cdot\text{mol}^{-1}$) and is promoted by a factor of 50–100 by a disaccharide attached to ring 4 (in vancomycin and eremomycin) and by a factor of ca. 1000 by an amino-sugar attached to the benzylic position of ring 6 in eremomycin. The dimerization process (which, as required for an exothermic association, appears to be costly in entropy) may be relevant to the mode of action of the antibiotics.

We have recently (1) built upon earlier work of Page and Jencks (2) and Jencks (3) in utilizing an equation which divides the observed free energy of binding (ΔG , $\text{kJ}\cdot\text{mol}^{-1}$) for a bimolecular association in aqueous solution ($A + B \rightarrow A\cdot B$) into several components:

$$\Delta G = \Delta G_{t+r} + \Delta G_r + \Delta G_h + \sum \Delta G_p + \Delta G_{vdw} + \Delta G_{conf}. \quad [1]$$

ΔG_{vdw} is the difference in the free energy of van der Waals interactions between the binding surfaces of A and B to each other and to solvent, and ΔG_{conf} is the difference in the conformational free energies between free and bound states. For the case where the binding surfaces of A and B have good complementarity, and where A and B can bind in the complex close to the conformational energy minima found for the components in free solution, we approximate the terms ΔG_{vdw} and ΔG_{conf} to zero (1). In the simpler equation which is then applicable (Eq. 2), ΔG_{t+r} corresponds essentially to the loss in translational and rotational entropy for a bimolecular association, and ΔG_r is the adverse change in entropy

due to the restriction of rotations upon association (both of these terms are expressed in terms of $T\Delta S$ at 300 K); ΔG_h is the favorable free energy change due to the hydrophobic effect (when hydrocarbon surface is removed from exposure to water upon association), and $\sum \Delta G_p$ is the favorable free energy change due to the interaction of pairs of polar functional groups which come together in the binding site (and summed over all such pairs of interactions). Where these last interactions are of ideal geometry, they represent *intrinsic* binding free energies (3).

$$\Delta G = \Delta G_{t+r} + \Delta G_r + \Delta G_h + \sum \Delta G_p. \quad [2]$$

In using this approach, we recognize that the derived parameters will be approximate only and may indeed vary from one environment to another (4). The analysis may be additionally complicated by cooperativity. It nevertheless seems worthwhile to attempt a semiquantitative approach even if only to give rough estimates of these parameters and to underscore any problems which the analysis may uncover.

For an intramolecular association, the term ΔG_{t+r} disappears and, in the idealized equation (Eq. 2), only three terms then remain. In intramolecular cases of complex interactions, such as protein folding, there will be conformational strain in the associated (folded) state and probably also better van der Waals packing in the folded state. In these cases, ΔG_{conf} and ΔG_{vdw} are, respectively, unfavorable and favorable toward folding, and the free energy of association is thus partitioned into a total of five terms (cf. Eq. 1).

Derivation of Some Free Energy Contributions

In an initial application of the method (1, 5) the binding of mono- and dipeptides to vancomycin group antibiotics was examined. This work underestimated the size of the hydrophobic effect in these systems and, consequently, greatly overestimated the amide–amide hydrogen bond strength. When such overestimates are used to analyze the balance of free energies involved in α -helix formation, the free energy cost of rotor restriction is thereby also overestimated. We have recently reconsidered our analysis, using the following approach (6). First, to calibrate the hydrophobic effect, the difference in free energy of binding of N -acetyl-D-Ala-D-Ala and N -acetyl-D-Ala-Gly to the antibiotic ristocetin A [-11.4 , -8.4 , and $-10.1 \text{ kJ}\cdot\text{mol}^{-1}$ from several different sources (1)] was taken in conjunction with a measurement of the difference in nonpolar surface area buried from solvent when the two ligands bind. This difference in surface areas (47 \AA^2) was measured in energy-minimized structures using MACROMODEL (7) with a water molecule of radius 1.4 \AA together with a high density of points on a sphere. These data give a hydrophobic contribution to binding of -0.18 to $-0.24 \text{ kJ}\cdot\text{mol}^{-1}\cdot\text{\AA}^{-2}$ (6), in good accord with the value (-0.23

The publication costs of this article were defrayed in part by page charge payment. This article must therefore be hereby marked "advertisement" in accordance with 18 U.S.C. §1734 solely to indicate this fact.

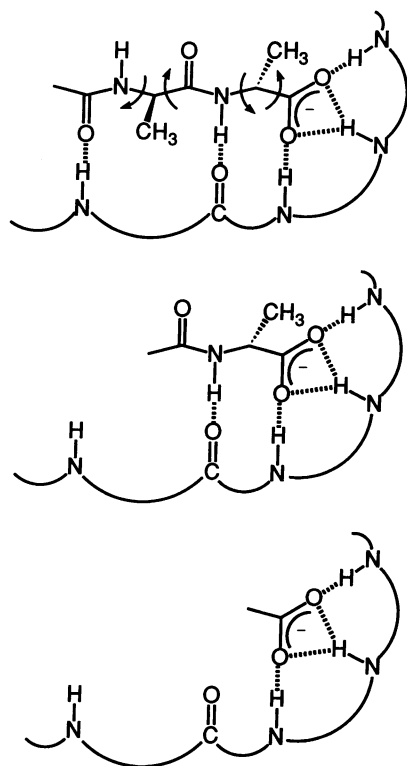


FIG. 1. Application of ligand extensions to the study of amide–amide hydrogen bonds in peptide–antibiotic complexes. Schematic representation of the interaction of *N*-Ac-D-Ala-D-Ala (Top), *N*-Ac-D-Ala (Middle), and acetate (Bottom) with the binding pocket of ristocetin A. Curved arrows identify the rotors restricted in the peptide backbone of *N*-Ac-D-Ala-D-Ala on binding to the antibiotic.

$\text{kJ}\cdot\text{mol}^{-1}$) recently found in protein engineering experiments on the stability of barnase (4). We have taken a value at the center of the experimental range, determined from six sets of data, and use $-0.2 \text{ kJ}\cdot\text{mol}^{-1}\cdot\text{\AA}^{-2}$ for the magnitude of the hydrophobic effect. Second, the entropic cost per rotor restricted when peptides bind to ristocetin A is taken to lie in the range $3.5\text{--}5.0 \text{ kJ}\cdot\text{mol}^{-1}$ ($T\Delta S$ at 300 K), where the lower value is that deduced from the entropic cost per rotor restricted in the crystallization of even-membered n -paraffins ($\text{C}_n\text{H}_{2n+2}$) (8), and the upper limit is derived from the entropic cost in the formation of small rings from linear hydrocarbons (2). [Since this upper limit corresponds to a process in which a covalent bond is formed (which in itself permits very little residual motion), the lower value of $3.5 \text{ kJ}\cdot\text{mol}^{-1}$ may be more appropriate for general use in associations where rotations are restricted by weaker (noncovalent) interactions.] If these

parameters are used to give values for ΔG_h and ΔG_r in Eq. 1, then it is possible to estimate ΔG_p values using the method of “ligand extension” (6) or “anchor principle” (3). For example, the free energy of binding of *N*-Ac-D-Ala-D-Ala over *N*-Ac-D-Ala to ristocetin A is $-11.4 \text{ kJ}\cdot\text{mol}^{-1}$ (1, 6). This increase in binding energy is achieved in association with the making of an extra amide–amide hydrogen bond, an increase in the surface area of hydrocarbon buried (by 85 \AA^2), but at the cost of restricting two peptide backbone rotations (Fig. 1). Therefore, we estimate the increase in binding free energy from the hydrophobic effect as $-17 \text{ kJ}\cdot\text{mol}^{-1}$, and the total cost of rotor restrictions as $7\text{--}10 \text{ kJ}\cdot\text{mol}^{-1}$ (the peptide backbone of the antibiotic is restricted both before and after binding). Since the adverse cost of the bimolecular association (ΔG_{i+r}) should be essentially the same for both of the ligands shown in Fig. 1 (since the ligands bind with similar exothermicities, and in these cases, ΔG_{i+r} depends only on the logarithm of the mass of the ligand; see below for details), then the ligand extension approach removes this parameter from Eq. 1, and we may write:

$$-11.4 = (7 \text{ to } 10) - 17 + \Delta G_p; \Delta G_p = -1.4 \text{ to } -4.4 \text{ kJ}\cdot\text{mol}^{-1},$$

where ΔG_p is the binding free energy of the amide–amide hydrogen bond in this system. The data from a total of nine sets of ligand extension experiments are presented in Table 1, where the data set also includes comparisons between the binding of acetate with *N*-Ac-D-Ala and with *N*-Ac-D-Ala-D-Ala (Fig. 1) (6, 9). It can be seen that seven of the derived ΔG_p values for the amide–amide hydrogen bond fall in the range -1.0 to $-4.6 \text{ kJ}\cdot\text{mol}^{-1}$, with only two much larger values (-12.5 and $-7.7 \text{ kJ}\cdot\text{mol}^{-1}$) falling outside this range. Of these last two, and possibly anomalously large values, two points are noteworthy. First, both include data for the ligand *N*-Ac-Gly-D-Ala (Table 1). Second, the $\Delta G_p = -7.7 \text{ kJ}\cdot\text{mol}^{-1}$ value is numerically less than the $\Delta G_p = -12.5 \text{ kJ}\cdot\text{mol}^{-1}$ value mainly because the former is averaged over two apparent hydrogen bond strengths, whereas the latter value is the apparent hydrogen bond strength associated with only the glycine extension. Thus, both of the exceptionally large values are associated with an *apparent* hydrogen bond strength of the same glycine extension, possibly because in this case binding is promoted by a factor for which appropriate allowance has not been made. We note that if these possible anomalies are ignored, and the data for all of the derived amide–amide hydrogen bond strengths are taken, then the average value over the nine data sets is $-4 \text{ kJ}\cdot\text{mol}^{-1}$. If the possibly anomalously large values are excluded from the averaging process, then an average strength of $-2.2 \text{ kJ}\cdot\text{mol}^{-1}$ is obtained.

Table 1. Estimation of the free energy of formation of the amide–amide hydrogen bond from ligand extension studies of peptide binding to ristocetin A

Ligand	$\Delta\Delta G^*$	$\Delta\Delta H^*$	$\Delta\Delta A_{np}$	$\Delta\Delta G_h^\dagger$	$\Delta\Delta G_r$	ΔN_{hb}^\ddagger	ΔG_p^\S
<i>N</i> -Ac-Ala-Ala/ <i>N</i> -Ac-Ala	-11.4	$+2.9 \pm 3.0$	85	-17	7-10	1	-2.9 ± 1.5
<i>N</i> -Ac-Gly-Ala/ <i>N</i> -Ac-Ala	-11.0	-3.4 ± 2.8	33	-7	7-10	1	-12.5 ± 1.5
<i>N</i> -Ac-Ala-Gly/ <i>N</i> -Ac-Ala	0	$+4.7 \pm 2.5$	39	-8	7-10	1	-1.0 ± 1.5
<i>N</i> -Ac-Gly-Gly/ <i>N</i> -Ac-Ala	+5.3	ND	9	-2	7-10	1	-1.2 ± 1.5
<i>N</i> -Ac-Ala/acetate	-11.4	ND	89	-18	7-10	1	-1.9 ± 1.5
<i>N</i> -Ac-Ala-Ala/acetate	-22.8	ND	174	-35	14-20	2	-2.4 ± 1.5
<i>N</i> -Ac-Gly-Ala/acetate	-22.4	ND	122	-24	14-20	2	-7.7 ± 1.5
<i>N</i> -Ac-Ala-Gly/acetate	-11.4	ND	128	-26	14-20	2	-1.3 ± 1.5
<i>N</i> -Ac-Gly-Gly/acetate	-6.1	ND	98	-20	14-20	2	-4.6 ± 1.5

ND, not determined.

*Data from ref. 9; acetate binding from ref. 1; binding of *N*-Ac-Gly-Gly, $K = 150 \pm 30 \text{ M}^{-1}$ at 295 K (unpublished results).

†Using $\Delta\Delta G/\Delta\Delta A_{np} = -0.2 \text{ kJ}\cdot\text{mol}^{-1}\cdot\text{\AA}^{-2}$.

‡Difference in the number of amide–amide hydrogen bonds.

§Amide–amide hydrogen bond energies.

Table 2. Estimates of average amide–amide hydrogen bond strengths (ΔG_p), based on differing values of ΔG_h and ΔG_r , from a comparison of the binding of peptide ligands to ristocetin A

Assumed ΔG_h , kJ·mol ⁻¹ ·Å ⁻²	Assumed ΔG_r , kJ·mol ⁻¹	Derived ΔG_p , kJ·mol ⁻¹
-0.15	3.5	-4 ± 2
-0.15	5.0	-7 ± 2
-0.20	3.5	-1 ± 2
-0.20	5.0	-4 ± 2

The above values are based on a particular assumed value for the hydrophobic effect ($-0.2 \text{ kJ}\cdot\text{mol}^{-1}\cdot\text{\AA}^{-2}$). This value is significantly larger than the value of $-0.125 \text{ kJ}\cdot\text{mol}^{-1}\cdot\text{\AA}^{-2}$ based on solvent transfer experiments (10), and at least part of this difference may arise because the smaller value does not allow for a favorable entropy of mixing in the solvent transfer experiments (11). Nevertheless, it would seem wise to also estimate ΔG_p values on the basis of a ΔG_h value closer to that long accepted on the basis of the solvent transfer data. This has been done in Table 2, for $\Delta G_h = -0.15 \text{ kJ}\cdot\text{mol}^{-1}\cdot\text{\AA}^{-2}$ in conjunction with rotor restrictions (ΔG_r) costing either 3.5 or 5.0 kJ·mol⁻¹. All of the estimates fall in the range $-(1 \text{ to } 7) \pm 2 \text{ kJ}\cdot\text{mol}^{-1}$ (Table 2). In this context, it is noteworthy that from the study of model peptides (12), many α -helices of moderate length (i.e., 15–50 residues) are formed with ΔG not far from zero in aqueous solution at physiological temperatures. When we consider that two rotors per residue are restricted within such helices, at a cost of *ca.* 3.5–5 kJ·mol⁻¹ per rotor, we are led to the conclusion that the average amide–amide hydrogen bond strength is less than $-(7 \text{ to } 10) \text{ kJ}\cdot\text{mol}^{-1}$ (since polyglycine will not form a helix, and assistance from a favorable side chain is required). However, alanine-rich helices do form with ΔG not far from zero, and O'Neil and DeGrado (13) have reported that within such moderately long helices, Ala stabilizes the helix over Gly by 3 kJ·mol⁻¹. Thus, the amide–amide hydrogen bond strength appears to be just sufficient to induce the rotor restrictions (7–10 kJ·mol⁻¹) with the helix-inducing aid ($-3 \text{ kJ}\cdot\text{mol}^{-1}$) of alanine. This reasoning gives a hydrogen bond strength of $-(4 \text{ to } 7) \text{ kJ}\cdot\text{mol}^{-1}$, consistent with the values cited above, and with values found for this bond (14), and for other neutral–neutral hydrogen bonds (15) from protein engineering experiments.

Phenomenon of Enthalpy/Entropy Compensation and Its Origins

The phenomenon of enthalpy/entropy compensation is well documented (see, for example, refs. 16–18) and of fundamental importance to molecular recognition phenomena. It is a universal phenomenon when the binding energy is comparable to the available thermal energy (kT). The origin of enthalpy/entropy compensation is found in the fact that associated states which lie in deep electrostatic wells have relatively little motion compared to the dissociated states in which the electrostatic attractions are removed or much reduced (Fig. 2a). Here, “deep” refers to potential wells where the electrostatic attractions are large compared to kT [where k is Boltzmann's constant and $T(K)$ is the temperature]. Conversely, if the endothermicity of dissociation is small (comparable to, or only a few times greater than, kT ; Fig. 2b), then there is much residual motion in the associated state, and the adverse entropy of the corresponding bimolecular association (ΔG_{t+r}) is only a relatively small fraction of the formal loss in ΔG_{t+r} corresponding to the formation of a rigid complex (5). The relevance of these considerations to bimolecular associations of biological interest may be illustrated by reference to an extreme case. The favorable free

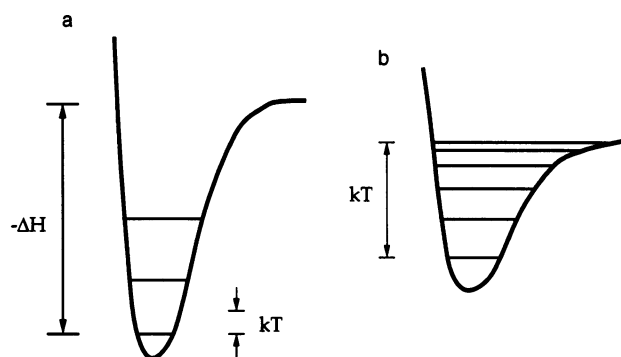


Fig. 2. Schematic illustration of a potential well in which the enthalpy of dissociation of a complex is large compared to kT (a) and where the enthalpy of dissociation is comparable to kT (b).

energy ($-28 \text{ kJ}\cdot\text{mol}^{-1}$ at 298 K) of transfer of pentane from an aqueous phase to bulk pentane can be achieved without a significant cost in translational and rotational entropy (i.e., without a significant ΔG_{t+r} term). Although much favorable free energy for the transfer is available, it occurs without a significant loss in translational and rotational entropy because the restraining intermolecular forces acting upon the transferred pentane molecule are not greater in pentane than in water (the transfer to pentane is actually endothermic by $2 \text{ kJ}\cdot\text{mol}^{-1}$) (19). In the case of biologically interesting associations, it is because of the increasing cost of an association in terms of ΔG_{t+r} as the endothermic barrier to dissociation increases that it is difficult to estimate the ΔG_{t+r} term and therefore why this term is advantageously eliminated from Eq. 1 by studying the binding of related ligands that bind with similar exothermicities (previous section).

The above considerations of enthalpy/entropy compensations have interesting implications for dissociations occurring with small vs. large enthalpic barriers. Consider a dissociation in which the separating polar functional groups become accessible to water even as the enthalpic cost of separating the polar functionalities is being paid and having a small enthalpic barrier of $x \text{ kJ}\cdot\text{mol}^{-1}$ (Fig. 3a). Contrast this process with the same dissociation but one in which the separating polar functional groups are inaccessible (or have poor accessibility) to solvent water in the transition state for dissociation (Fig. 3b). Other things being equal, this latter process will have an enthalpic barrier greater than $x \text{ kJ}\cdot\text{mol}^{-1}$, because in the transition state it is more akin to a gas-phase dissociation, and there is poorer stabilization of the polar functional groups. Because of the greater enthalpic cost to attain the transition state for dissociation in this case, the complex will on average undergo lower amplitude breathing motions and with greater probability occupy the region of space corresponding to the bottom of the well where the density of energy states is lower. The consequence is that the complex is now less favored entropically than in Fig. 3a (i.e., it is

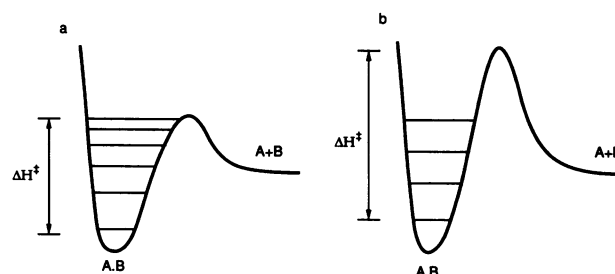


Fig. 3. Schematic illustration of dissociation processes in which there is a small enthalpic barrier to dissociation (a) and a large enthalpic barrier to dissociation (b).

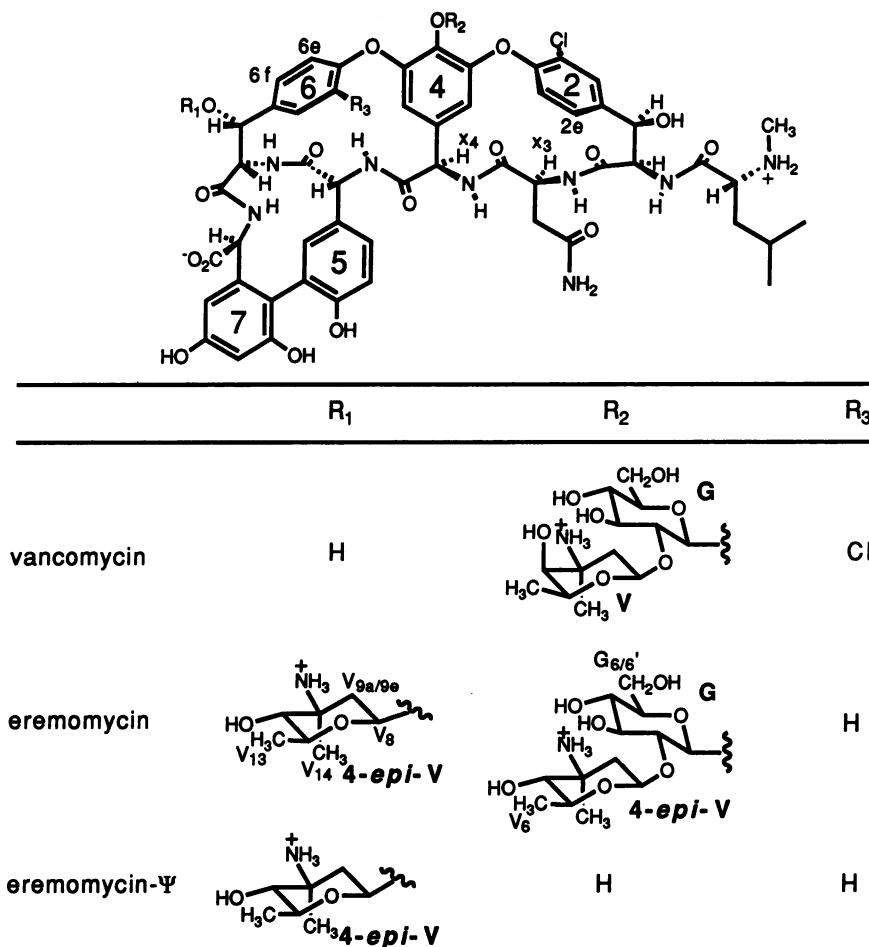


FIG. 4. Structures of the antibiotics vancomycin, eremomycin, and eremomycin- ψ .

“tighter” in Fig. 3*b*). However, this adverse effect is offset by further enthalpic stabilization (in Fig. 3*b* over 3*a*) due to larger electrostatic attractions associated with shorter distances (on average) between the polar functionalities in the presence of the large barrier. In summary, a lack of access to solvent water in thermally accessible motions can lead to a more favorable thermodynamic enthalpy of binding at a cost of a more adverse thermodynamic entropy of binding. It follows that the adverse entropic term ΔG_{t+r} for the association step should be larger in Fig. 3*b* than in 3*a*.

Dimerization of Vancomycin Group Antibiotics

A situation which corresponds to Fig. 3*b* has been probed experimentally by determining the thermodynamic parameters for dimerization of some vancomycin group antibiotics (vancomycin, eremomycin, eremomycin- ψ , ristocetin A, and ristocetin- ψ) (20). The antibiotic structures are given in Figs. 4 and 5, and the hydrogen-bonded dimer structure is depicted in Fig. 6. The values of ΔH_{dim} and $T\Delta S_{dim}$, derived from proton NMR studies of the temperature variation of the dimerization constant, are summarized in Table 3. In the dimer structures, the amide NHs (of residues 5 and 6) and the amide carbonyl groups (of residues 3 and 5), which are involved in the formation of four intermolecular amide–amide hydrogen bonds (between the two halves of the dimer), are relatively inaccessible to solvent because of the steric bulk of the surrounding aromatic rings and sugars. Therefore, as these hydrogen bonds stretch in the motion leading to dissociation, the polar groups are not well solvated by water, such that the transition state for dissociation is enthalpically destabilized relative to both the dimer and the monomer.

The presence of a large free energy barrier (mainly enthalpic) to dissociation of the dimer of eremomycin is consistent with (but not proved by) the occurrence of two forms of the dimer (20, 21, *) in equilibrium with each other at room temperature. The half-life for interconversion of the two forms of the dimer is long compared to the NMR time scale. If it is assumed that the rate determining step in the interconversion of the two forms of the dimer is dissociation of dimer to monomer (i.e., that the interconversion of the two forms of dimer occurs through monomer), then the coalescence temperature (308 K) of the two sets of signals indicates a free energy barrier to dissociation of the dimer of *ca.* 60 kJ·mol⁻¹. However, if the two forms of the dimer can interconvert without dissociation, then the dissociation barrier cannot of course be inferred from these data. Nevertheless, a large dimer dissociation barrier (*ca.* 60 kJ·mol⁻¹) is independently found for the ristocetin A/di-Ac-Lys-D-Ala-D-Ala complex, since in this case slow exchange with the monomer complex can be directly observed (21). If the model under discussion is appropriate (Fig. 3*b*), this barrier should be largely enthalpic.

In accord with the model (i.e., Fig. 3*b* being appropriate, not Fig. 3*a*), the experimental enthalpies for the dimerization

*In earlier work (20, 21), we had been unable to distinguish between two sets of dimer proton resonances arising either from a single asymmetric dimer or two different forms of the dimer. This was because the two sets of dimer proton resonances were of equal intensity. However, we have now observed (J.P.M., unpublished) that these two sets of resonances in the eremomycin/di-Ac-Lys-D-Ala-D-Ala dimer complex are of unequal intensity. This observation precludes the existence of a single asymmetric dimer but is in accord with the existence of two different dimer structures.

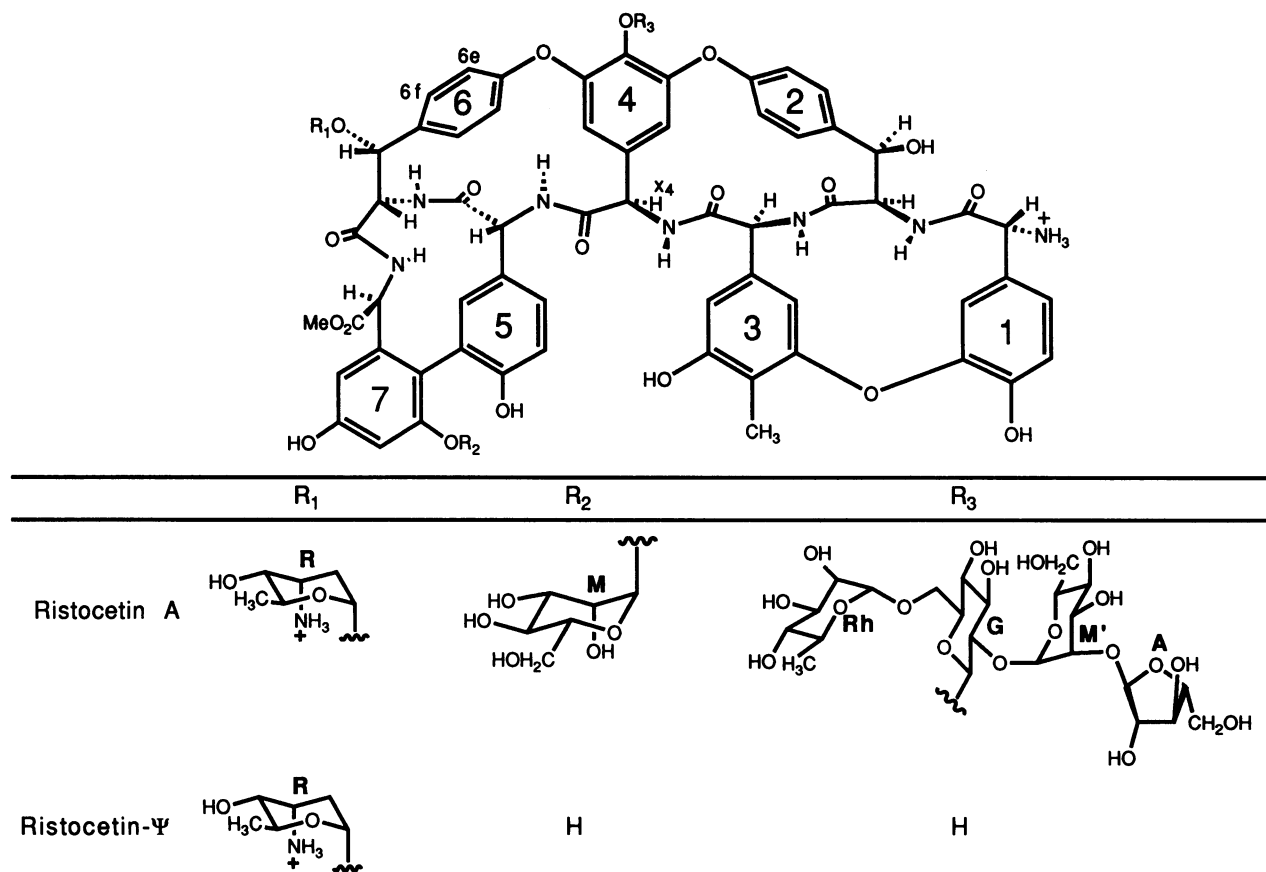


FIG. 5. Structures of the antibiotics ristocetin A and ristocetin-Ψ.

of the vancomycin group antibiotics are relatively large (-36 to -51 $\text{kJ}\cdot\text{mol}^{-1}$, Table 3; accordingly, the enthalpic barriers to dissociation must be at least equal and opposite in sign to these numbers, or even more positive). In the dimerization of vancomycin, the main factors which appear likely to promote the association can be identified:

(i) Four amide–amide hydrogen bonds are formed due to interaction between the peptide backbone of one antibiotic molecule and the other (cf. Fig. 6). There is also the possibility for the formation of another amide–amide hydrogen bond between an NH of the side chain of residue 3 (asparagine) and the carbonyl oxygen of residue 6 in the other half

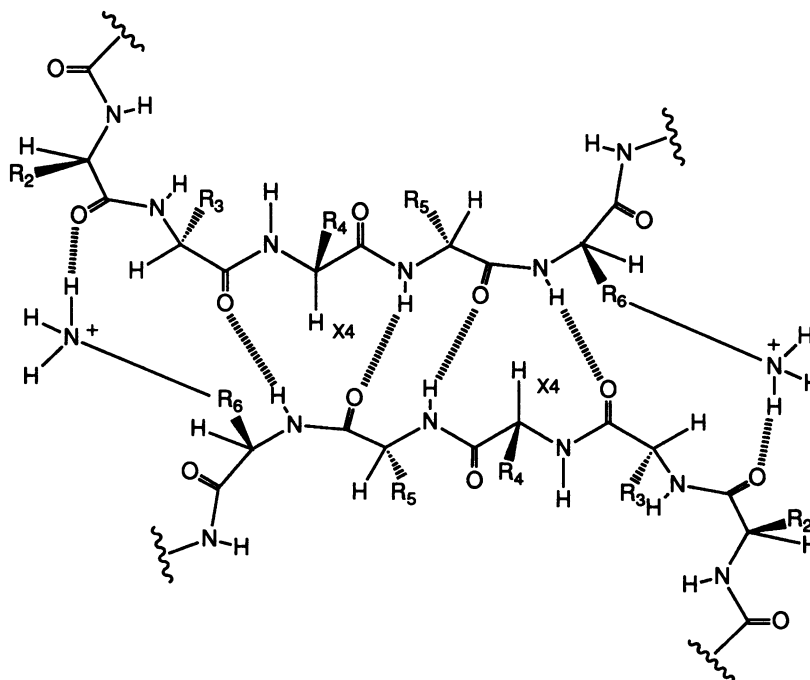


FIG. 6. Hydrogen bonding interactions between the two halves of the dimer in vancomycin group antibiotics.

Table 3. Dimerization constants for a number of different glycopeptide antibiotics and their derivatives

Compound	K_{dim} , M ⁻¹ (298 K)	ΔH_{dim} , kJ·mol ⁻¹	$T\Delta S_{\text{dim}}$,* kJ·mol ⁻¹
Eremomycin	$>1 \times 10^6$ [†]	—	—
Eremomycin- Ψ	1.5×10^4	-51 ± 3	-27 ± 3
Ristocetin	$\approx 2 \times 10^3$ [‡]	—	—
Ristocetin- Ψ	50	-37 ± 6	-28 ± 7
Vancomycin	700	-36 ± 2	-20 ± 5

ΔH_{dim} and $T\Delta S_{\text{dim}}$ values were calculated from van't Hoff plots of $\ln(K_{\text{dim}})$ versus $1/T$.

*Calculated at 298 K.

[†]Estimated from the absence of any signals assignable to monomer in the ¹H NMR spectrum at 1 mM concentration.

[‡]Estimated from the relative proportions of monomer and dimer signals at different concentrations between 1.5 and 15 mM ristocetin.

of the dimer. Although no experimental evidence is currently available for the formation of this hydrogen bond, potentially occurring twice over in the dimer, the possibility of its occurrence gives a total maximum number of amide–amide hydrogen bonds as six.

(ii) Inspection of molecular models (or use of molecular graphics) reveals an interaction where two –C–H bonds of ring 6 are orientated almost perpendicularly into the π -electron density of benzene ring 4. This interaction occurs twice over in the dimer. Experimental support for its occurrence is available since the protons (6e and 6f, Figs. 4 and 5) of these two C–H bonds move markedly to high field upon dimer formation—for example, by 2.3 and 0.7 ppm, respectively, in the formation of the ristocetin A dimer when complexed to the cell wall tripeptide analogue di-Ac-Lys-D-Ala-D-Ala (21).

(iii) In the dimerization process, a relatively large surface area of hydrocarbon is removed from exposure to water. This area can be estimated by rolling a water molecule of radius 1.4 Å over the hydrophobic surface of both the monomer and the dimer and then subtracting the exposed surface area of the dimer from twice that of the monomer. The value obtained in this way is 290 Å² for aglucovancomycin [i.e., vancomycin with the disaccharide R₂ removed (Fig. 4)].

(iv) In the dimer, the disaccharide attached to ring 4 of vancomycin (Fig. 4) can interact with the corresponding disaccharide unit in the other half of the dimer. Because the dimerization constant of aglucovancomycin (which lacks this disaccharide unit) is weaker than that of vancomycin, it cannot be measured with the same precision as that of vancomycin, but the disaccharide unit promotes binding by a factor of *ca.* 50.

The dimerization constant of vancomycin is 700 M⁻¹, and the process is exothermic by 36 kJ·mol⁻¹ (Table 3). Using the value of *ca.* $-0.20 \text{ kJ}\cdot\text{mol}^{-1}\cdot\text{Å}^{-2}$ for the hydrophobic effect, then factor *iii* clearly gives a very large free energy contribution to binding ($-58 \pm 20 \text{ kJ}\cdot\text{mol}^{-1}$), but this favorable free energy is expected to be almost completely entropy driven. For example, when 209 Å² of hydrocarbon surface area is removed from exposure to water in the transfer of ethylbenzene from water to bulk ethylbenzene, the process is exothermic by only 1.9 kJ·mol⁻¹ at 298 K, out of a total favorable free energy change of $-26 \text{ kJ}\cdot\text{mol}^{-1}$ (19, 22, 23). Factor *ii* is a possible source of some exothermicity, since edge-to-face interactions in aromatic rings are known to be enthalpically favorable and occur, for example, in crystalline benzene. Since the dimerization is promoted by a factor of *ca.* 50 by the disaccharide unit (factor *iv*), this contribution is *ca.* $-10 \text{ kJ}\cdot\text{mol}^{-1}$ to the free energy of binding at 298 K. The overall structure of the dimer indicates that the main interaction between the two units of the disaccharide in the dimer is between the two glucose units. Any hydrogen bonds formed

between these units should involve only sugar OH groups, which are not expected to be important contributors to exothermicity in the present context. Two glucose molecules can, however, interact via their hydrophobic faces (the axial C–H groups of their α -faces) and thereby promote binding entropically.

The above arguments suggest that large exothermicities are unlikely to arise from factors *iii* and *iv*. Therefore, the large exothermicity is likely to be mainly associated with some combination of the formation of several amide–amide hydrogen bonds (factor *i*) and σ – π aromatic interactions (factor *ii*). With regard to factor *i*, there is not consistent supporting calorimetric evidence for significant exothermicity where an extra amide–amide hydrogen bond is made in binding *N*-acetyl-dipeptides, relative to *N*-acetyl-mono-peptides, to ristocetin A (Table 1, first three rows of column 3, $\Delta\Delta H = +2.9$, -3.4 , and $+4.7 \text{ kJ}\cdot\text{mol}^{-1}$) nor in the $\Delta\Delta H$ values ($+0.2$, $+1.4$, and $+5.0 \text{ kJ}\cdot\text{mol}^{-1}$) for precisely the same changes in peptide ligands but binding to the antibiotic vancomycin (9). On the other hand, Scholtz *et al.* (12) have reported that ΔH per residue for α -helix formation lies in the range -3.8 to $-5.5 \text{ kJ}\cdot\text{mol}^{-1}$ in helices of moderate length (12), presumably largely associated with a favorable enthalpy of amide–amide hydrogen bond formation. It is possible that the origin of these apparent inconsistencies may lie, at least in part, in entropy/enthalpy compensation (Fig. 3); the amide–amide hydrogen bonds near the center of the dimer structure (Fig. 4), and near the center of extended α -helices, may be more shielded from water in breathing motions (and therefore associated with greater exothermicity) than is the corresponding bond at the terminus of an *N*-acetyl-dipeptide binding to the antibiotics.

We note that the entropic cost *specifically for the bimolecular association* (in terms of $T\Delta S$ at 300 K, and to a good approximation $\Delta G_{\text{t+r}}$) for the dimerization of vancomycin is given by the experimental entropy change for dimerization ($T\Delta S = -20 \pm 5 \text{ kJ}\cdot\text{mol}^{-1}$ at 298 K, Table 3) minus any favorable change in $T\Delta S$ due to specific interactions generated in dimerization. Since for these particular dimerizations it has been argued that the main source of exothermicity will derive from the hydrogen bonds and the σ – π interactions (see above), it is a corollary of this conclusion that the favorable entropy changes should largely originate from the hydrophobic effect ($58 \pm 20 \text{ kJ}\cdot\text{mol}^{-1}$) and the disaccharide ($10 \text{ kJ}\cdot\text{mol}^{-1}$). An estimate of $\Delta G_{\text{t+r}}$ is therefore:

$$\Delta G_{\text{t+r}} = -20 - 68 = -88 \pm 40 \text{ kJ}\cdot\text{mol}^{-1},$$

where $\pm 40 \text{ kJ}\cdot\text{mol}^{-1}$ reflects both the experimental errors and the assumptions in the approach. The formal entropic cost in forming a *rigid* dimer of this molecular weight is *ca.* $-72 \text{ kJ}\cdot\text{mol}^{-1}$ (1, 6). Since the dimer is certainly not rigid, and will retain some residual motion, $\Delta G_{\text{t+r}}$ appears to be overestimated by the above arithmetic. However, even applying the lower limit for the hydrophobic effect, the loss in translational and rotational entropy in formation of the vancomycin dimer appears to be large—i.e., it is better modeled by a strongly exothermic interaction than by a weakly exothermic one (Fig. 2).

The promotion of dimerization of vancomycin by a factor of *ca.* 50 by the ring 4 disaccharide (see above) and of eremomycin by a factor of at least 100 by its ring 4 disaccharide (Table 3) may imply a physiological role for the dimerization. This possibility is made more intriguing by the observation that the amino-sugar attached to the benzylic position of ring 6 of eremomycin promotes its dimerization (relative to the otherwise structurally extremely similar vancomycin) by a factor of at least 10³ (Table 3). Thus, the sugars in these molecules appear to have structures, and locations, which strongly promote dimerization. Since eremomycin

acts as an antibiotic with a lower minimum inhibitory concentration than vancomycin, despite the fact that the latter has the larger binding constant to the cell wall analogue *N*-di-Ac-Lys-D-Ala-D-Ala (24), antibacterial action may be promoted by dimerization.

We thank SERC, the Upjohn company (Kalamazoo), and Schering (U.K.) for financial support. The work was carried out within the Cambridge Centre for Molecular Recognition.

1. Williams, D. H., Cox, J. P. L., Doig, A. J., Gardner, M., Gerhard, U., Kaye, P. T., Lal, A. R., Nicholls, I. A., Salter, C. J. & Mitchell, R. C. (1991) *J. Am. Chem. Soc.* **113**, 7020–7030.
2. Page, M. I. & Jencks, W. P. (1971) *Proc. Natl. Acad. Sci. USA* **68**, 1678–1683.
3. Jencks, W. P. (1981) *Proc. Natl. Acad. Sci. USA* **78**, 4046–4050.
4. Serrano, L., Neira, J.-L., Sancho, J. & Fersht, A. R. (1992) *Nature (London)* **356**, 453–455.
5. Williams, D. H. (1991) *Aldrichimica Acta* **24**, 71–80.
6. Searle, M. S., Williams, D. H. & Gerhard, U. (1993) *J. Am. Chem. Soc.*, in press.
7. Mohamadi, F., Richards, N. G. J., Guida, W. C., Liskamp, R., Lipton, M., Caufield, C., Chang, G., Hendrickson, T. & Still, W. C. (1990) *J. Comput. Chem.* **11**, 440–467.
8. Searle, M. S. & Williams, D. H. (1993) *J. Am. Chem. Soc.*, in press.
9. Rodriguez-Tebar, A., Vasquez, D., Perez-Velazquez, J. L., Laynez, J. & Wadso, I. J. (1986) *J. Antibiotics* **39**, 1587–1583.
10. Chothia, C. & Janin, J. (1975) *Nature (London)* **256**, 705–708.
11. Sharp, K. A., Nicholls, I. A., Fine, R. F. & Honig, B. (1991) *Science* **252**, 106–109.
12. Scholtz, J. M., Marqusee, S., Baldwin, R. L., York, E. J., Stewart, J. M., Santoro, M. & Bolen, D. W. (1991) *Proc. Natl. Acad. Sci. USA* **88**, 2854–2858.
13. O'Neil, K. T. & DeGrado, W. F. (1990) *Science* **250**, 646–649.
14. Shirley, B. A., Stanssens, P., Hahn, U. & Pace, C. M. (1992) *Biochemistry* **31**, 725–732.
15. Fersht, A. R. (1987) *Trends Biochem. Sci.* **12**, 301–304.
16. Jencks, W. P. (1975) *Adv. Enzymol.* **43**, 219–410.
17. Lumry, R. & Rajender, S. (1970) *Biopolymers* **9**, 1125–1227.
18. Miklavc, A., Kocjan, D., Mavri, J., Koller, J. & Hazdi, D. (1990) *Biochem. Pharmacol.* **40**, 663–669.
19. Doig, A. J. & Williams, D. H. (1991) *J. Mol. Biol.* **217**, 389–398.
20. Gerhard, U., Mackay, J. P., Maplestone, R. A. & Williams, D. H. (1993) *J. Am. Chem. Soc.*, in press.
21. Waltho, J. P. & Williams, D. H. (1989) *J. Am. Chem. Soc.* **111**, 2475–2480.
22. McAuliffe, C. (1966) *J. Phys. Chem.* **70**, 1267–1275.
23. Baldwin, R. L. (1986) *Proc. Natl. Acad. Sci. USA* **83**, 8069–8072.
24. Good, V. M., Gwynn, M. N. & Knowles, D. J. C. (1990) *J. Antibiotics* **43**, 550–555.